Available online at www.sciencedirect.com
ScienceDirect
Journal of Molecular Graphics and Modelling 26 (2007) 69–85
Journal of Molecular Graphics and Modelling
www.elsevier.com/locate/JMGM

Molecular characterization and phylogenetic analysis of BjussuMP-I: A RGD-P-III class hemorrhagic metalloprotease from *Bothrops jararacussu* snake venom☆

Maurício V. Mazzi [a,1], Angelo J. Magro [b,1], Saulo F. Amui [a], Clayton Z. Oliveira [a], Fábio K. Ticli [a], Rodrigo G. Stábeli [c], André L. Fuly [d], José C. Rosa [e], Antônio S.K. Braz [f], Marcos R.M. Fontes [b], Suely V. Sampaio [a,*], Andreimar M. Soares [a,*]

[a] *Departamento de Análises Clínicas, Toxicológicas e Bromatológicas, Faculdade de Ciências Farmacêuticas de Ribeirão Preto, FCFRP, Universidade de São Paulo, USP, Ribeirão Preto, SP, Brazil*
[b] *Departamento de Física e Biofísica, Instituto de Biociências, UNESP, Botucatu, SP, Brazil*
[c] *Instituto de Pesquisa em Patologia Tropical, Universidade de Rondônia, UNIR, Porto Velho, RO, Brazil*
[d] *Instituto de Biologia, Departamento de Biologia Celular e Molecular, Universidade Federal Fluminense, UFF, Niterói, RJ, Brazil*
[e] *Departamento de Biologia Celular e Molecular e Bioagentes Patogênicos and Centro de Química de Proteínas, FMRP-USP, Ribeirão Preto, SP, Brazil*
[f] *Departamento de Genética, Instituto de Biociências, UNESP, Botucatu, SP, Brazil*

Received 7 June 2006; received in revised form 20 September 2006; accepted 21 September 2006
Available online 28 September 2006

Abstract

Snake venom metalloproteases (SVMPs) embody zinc-dependent multidomain enzymes responsible for a relevant pathophysiology in envenomation, including local and systemic hemorrhage. The molecular features responsible for hemorrhagic potency of SVMPs have been associated with their multidomains structures which can target these proteins them to several receptors of different tissues and cellular types. BjussuMP-I, a SVMP isolated from the *Bothrops jararacussu* venom, has been characterized as a P-III hemorrhagic metalloprotease. The complete cDNA sequence of BjussuMP-I with 1641bp encodes open reading frames of 547 amino acid residues, which conserve the common domains of P-III high molecular weight hemorrhagic metalloproteases: (i) pre-pro-peptide, (ii) metalloprotease, (iii) disintegrin-like and (iv) rich cysteine domain. BjussuMP-I induced lyses in fibrin clots and inhibited collagen- and ADP-induced platelet aggregation. We are reporting, for the first time, the primary structure of an RGD-P-III class snake venom metalloprotease. A phylogenetic analysis of the BjussuMP-I metalloprotease/catalytic domain was performed to get new insights into the molecular evolution of the metalloproteases. A theoretical molecular model of this domain was built through folding recognition (threading) techniques and refined by molecular dynamics simulation. Then, the final BjussuMP-I catalytic domain model was compared to other SVMPs and Reprolysin family proteins in order to identify eventual structural differences, which could help to understand the biochemical activities of these enzymes. The presence of large hydrophobic areas and some conserved surface charge-positive residues were identified as important features of the SVMPs and other metalloproteases.

Keywords: *Bothrops jararacussu*; Snake venom hemorrhagic metalloprotease; cDNA; Phylogenetic analysis; Molecular evolution; Structural analysis

1. Introduction

Snake venoms comprise a complex mixture of pharmacological and toxic active components able to affect several biological systems. The toxic effects of snake venoms are associated with different actions of the major neurotoxins and hemorrhagins. Local and systemic hemorrhagic effects are due to synergic actions of proteolytic enzymes, such as metalloproteases (MPs) and serine-proteases (SPs) [1]. The local

Abbreviations: BjussuMP-I, *Bothrops jararacussu* hemorrhagic metalloprotease I; MP, metalloprotease; PTC-aa, phenylthiocarbamil amino acids; SVMPs, snake venoms metalloproteases

☆ The sequence data of BjussuMP-I reported in this paper has been submitted to the GenBank under accession no. DQ408681.

* Corresponding authors. Fax: +55 16 3602 4725.
E-mail addresses: suvilela@fcfrp.usp.br (S.V. Sampaio), andreims@fcfrp.usp.br (A.M. Soares).

[1] These authors contributed equally to the work.

1093-3263/$ – see front matter © 2006 Elsevier Inc. All rights reserved.
doi:10.1016/j.jmgm.2006.09.010

pathophysiology manifestation of *Bothrops* genus envenomation includes necrosis, blistering, and edema [2–5].

The pathogenesis of venom-induced hemorrhage involves biochemical and biophysical alterations on capillary vessel structure by the action of MPs, which selectively cleave key peptide bonds of basement membrane components such as laminin, fibronectin and type IV collagen [3,5]. Thus, different mechanisms are involved in extravasion of blood and erythrocytes through gaps or intercellular junctions of endothelial cells [5].

Some secondary symptoms including cardiovascular shock may occur as a characteristic of severe envenomations. Systemically, α and β fibrinogenases (MPs and SPs) affect the blood coagulation in different ways, displaying procoagulant, fibrinogen clotting, fibrin and/or fibrinogenolysis and platelet modulations [6–10].

The fact some viper venoms may cause bleeding led many researchers to find out which groups of toxins can accelerate the process of blood coagulation or inhibit it [10]. Despite toxicological interests, some compounds such as snake venom thrombin-like enzymes (SVTLE) and metalloproteases (SVMPs) have been proved to be therapeutically useful as anticoagulants or for the development of diagnostic reagents [11]. During the last decades, some snake venom toxins have been shown to mimic/inhibit physiologically the platelets by interacting/degrading the major integrins of this system, namely Ib-IX-V, von Willebrand factor, $\alpha_2\beta_1$ and αIIbβ3/IIb-IIIa [7,12–14].

Recent studies have also used venom SVMPs to explore the cellular metabolism of many other cells. HF3, a P-III class metalloprotease from *Bothrops jararaca* and its recombinant disintegrin-like/cystein rich domains (DC-HF3), for example, activated phagocytosis by interacting with integrins $\alpha_M\beta_2$, which are central receptors located on leukocytes surface [4]. Cellular adhesion and apoptosis have been recently studied by using a 106 kDa SVMP from *Vipera lebetina*, which promoted both endothelial cell alterations and cell apoptosis [15]. Jararhagin, a P-III class toxin from *B. jararaca* venom [16] was extensively studied as a potent inhibitor of collagen-induced platelet aggregation via cleavage of $\alpha_2\beta_1/\beta_1$ subunit [7,17,18].

Snake venom metalloproteases (SVMPs) are zinc-dependent enzymes members of the Reprolysin subfamily, which include the ADAMs (*a d*isintegrin and *m*etalloproteinase) domains. Functional and structural characteristics of SVMPs have been extensively studied providing new insights into the biochemistry and pharmacology of these multidomain proteins [24]. They are responsible for a relevant pathophysiology in envenomation, including local and systemic hemorrhage. Alteration of basal membrane components and interactions with some factors of the coagulation pathway are the main actions of these classes of enzymes [3,5]. Moreover, these compounds were also demonstrated to be an important tool to understand signaling mechanisms either apoptosis or other cell adhesion alterations involved in wound healing and tumoral metastasis. These effects were recently observed with VLAIP and BaG from *V. lebetina* and *Bothrops alternatus*, respectively [15,20].

SVMPs are synthesized in the venom gland as large multidomain proteins, including a proenzyme and a conserved zinc-protease domains [1]. They are secreted as preproenzymes and contain additional regulatory modules, which are responsible for interactions with the extracellular matrix and integrins. Mature P-I class proteins have only a metalloprotease domain, whereas P-II, P-III, and P-IV classes have disintegrin or disintegrin-like, cysteine-rich, and lectin-like domains found close to the carboxyl end of the protease, respectively [1,2].

Important correlations have been established between hemorrhage and structural domains P-III class SVMPs, which are the most potent hemorrhagic toxins isolated from snake venoms. Some additional domains of these proteins (disintegrin-like and cysteine-rich) act in local and systemic hemmorrhage [2,19]. Other comparative structural studies of hemorrhagic and non-hemorrhagic SVMPs have suggested that, in addition to disintegrin and cysteine residues, *N*-glycosylation with post-translational modification site (NCSY, NCSK) may contribute to hemorrhagic potency of some MPs [3,19,21]. Disintegrins are low molecular weight non-enzymatic venom components containing RGD or KGD sequences, reported as the main structures, which bind to platelet surface integrins and modulate platelet aggregation by different mechanisms [7]. However, most of disintegrin-like domains of the metalloproteases do not have an RGD sequence. With some exceptions, hemorrhagic and non-hemorrhagic SVMPs have a conserved ECD sequence near the region where an RGD sequence is found in the ‘‘true’’ disintegrins [7].

Recently, we isolated a 60 kDa hemorrhagic metalloprotease, BjussuMP-I, from *Bothrops jararacussu* snake venom [22]. BjussuMP-I exhibited proteolytic activity on fibrinogen that was completely inhibited by chelant agents. Because platelets play crucial role in hemostasis and are targets of metalloproteases disintegrin-like/disintegrins, we have investigated BjussuMP-I as an inhibitor of platelet aggregation. We also report the deduced full length sequence of BjussuMP-I by cDNA cloning, and, for the first time, the primary structure of an RGD-P-III class snake venom metalloprotease.

In addition, a phylogenetic analysis of the BjussuMP-I metalloprotease/catalytic domain was done to find out new insights into the molecular evolution of the metalloproteases. A theoretical model of this domain was also built through folding recognition (threading) techniques and refined by a molecular dynamics simulation. Then, the final BjussuMP-I catalytic domain model was compared to the corresponding domains present in other SVMPs and Reprolysin family proteins in order to identify eventual structural differences, which could help to understand the biochemical activities of these enzymes.

2. Materials and methods

2.1. Materials

BjussuMP-I and BthA-I-PLA_2 were purified from *B. jararacussu* snake venom using the methodology previously described [22,23].

2.2. Fibrinolytic activity of BjussuMP-I

Plates containing fibrin clots were prepared by the method of Leitão et al. [24] with some modifications. The methodology consists of mixing equal volumes of 0.3% fibrin and 0.95% agarose solutions, both dissolved in 50 mM barbital buffer (pH 7.8, 1.66 mM $CaCl_2$, 0.68 mM $MgCl_2$ and 93.96 mM NaCl). The fibrinogen–agarose mixture was coagulated with 80 μL thrombin (1 μg/μL) in glass Petri dishes 90 mm × 1.5 mm. After 30 min at 4 °C an adequate number of wells (5 mm in diameter) were dug. To determine fibrinolytic activity, 30 μL aliquots of crude *B. jararacussu* venom (Bioagents Serpentarium, Batatais, SP) and BjussuMP-I were added to each well, the plate incubated, and areas of lysis quantified after 12 h at 37 °C.

2.3. Platelet aggregation assay

In this assay, the procedure described by Andrião-Escarso et al. [22] was used. Platelet rich plasma (PRP) was prepared from citrated rabbit blood (0.31%, w/v) by centrifugation (360 × *g*/12 min) at room temperature. PRP samples obtained as above were centrifuged at 1370 × *g* for 20 min and the platelet pellets were suspended in a calcium-free Tyrode's solution containing 0.35% (w/v) bovine serum albumin (BSA) and 0.1 mM EGTA (final concentration), pH 6.5, and washed twice by centrifugation. The final pellet was then suspended in Tyrode-BSA, pH 7.5, without EGTA. The suspension was adjusted to give (3–4) × 10^5 platelets/μL. Platelet aggregation was measured by turbidimetry using a Whole Blood Lumi-Aggregometer, Chrono-Log Corporation. Assays were performed at 37 °C in siliconized glass cells using 200 μL of PRP, under stirring, and aggregation was triggered after pre-incubation for 2 min with aliquots of *B. jararacussu* metalloprotease (BjussuMP-I) or acidic PLA_2 (BthA-I-PLA_2) in the presence of 1.0 mM $CaCl_2$ (final concentration). Control experiments were done using the platelet agonists alone (ADP or collagen).

2.4. Amino acid analysis

Amino acid composition was determined using a LDC Analytical HPLC (LDC-Thermo Separation Products). Previously, samples (0.3–0.6 μg/μL) of BjussuMP-I were hydrolyzed with 6 M HCl/0.5% phenol (v/v) for 24 h in vapor phase. The hydrolyzed BjussuMP-I was derivatized to phenylthiocarbamyl with 7:1:1:1 methanol:water:TEA:PITC (v/v/v/v) and the PTC-aa were separated by reverse phase HPLC on a C-18 column (Picotag 3.9 mm × 150 mm) from Waters, using a non-linear gradient from 8 to 52%B with 0.14 M of sodium acetate buffer pH 5.8 as solvent A and, acetonitrile:H_2O (60:40 v/v) as buffer B, at flow rate of 1.0 mL/min, temperature of 38 °C with effluent monitored at 254 nm. Data were analyzed by LC Talk software (Thermo Separation products) after standard calibration with amino acid mixture from Pierce Chemical Co.

2.5. Protein and DNA sequencing, design and synthesis of oligonucleotide probes

Briefly, BjussuMP-I (100 pmol) was reduced with 45 mM DTT for 1 h at 56 °C, followed by alkylation with 100 mM iodoacetamide for 3 h at 25 °C. N-terminal amino acid sequencing of BjussuMP-I was performed using a Procise protein sequenator model 491 (Perkin-Elmer Applied Biosystem Division, Foster City, CA) by automatic Edman degradation reaction using gas-phase chemistry with on-line identification of phenylthiohydantoin derivatives.

The primers used [5′-GGAAAAGATTATGACCGAGA-3′ and 5′-TTGTTGGTTA GGCATGG(T/A)-3′] were designed according to N and C-terminal sequences of other snake venom MPs from class III and N-terminal sequence of BjussuMP-I. Total RNA was extracted from *B. jararacussu* venomous glands using the Trizol™ method as specified by the manufacturer. Later on, 5 μg of total RNA was submitted to the reverse transcription reaction for synthesis of the first cDNA strand of the toxin in the presence of reverse transcriptase and oligo dT for 1 h at 42 °C. The second strand was synthetized using 2 μL of the above volume, combined with general and specific primers in order to allow the enzyme to amplify the wanted genes.

The final product was analyzed for size after amplification on 1.5% agarose gel stained with ethidium bromide. Purification of the PCR product was then carried out using Concert Rapid PCR Purification System (Gibco BRL) kit, according to the manufacturer's specifications. The sequencing reaction was led from the purified product using the ABI Prism® Big Dye™ Terminator Cycle Sequencing Ready Reaction kit (Perkin-Elmer), while electrophoresis was run in the ABI Prism 377 DNA Sequencer (Perkin-Elmer) apparatus, using a 4% polyacrylamide gel plus 6 M urea. Electrophoresis was run at 1500 V, 51 °C, for 7 h. The electrophorogram obtained were analyzed with the ABI Analysis Data Collection program and the sequences were then analyzed with the Sequencer software, version 3.1.

2.6. Sequence identification in databases

The amino acid sequence of the BjussuMP-I metalloprotease domain was used as a probe to search for homologous sequences in the NCBI (http://www.ncbi.nlm.nih.gov) and UniProt databases (http://www.pir.uniprot.org). The BLAST P was used to select sequences in the first database, with a BLOSUM45 distance matrix and default parameters. The minimum e-value of the sequences selected using the BLASTp was 1e-28. UniProt database searching was executed through the Pfam website (http://www.sanger.ac.uk/Software/Pfam/). All the identified protein sequences and their respective data base identification codes are shown in Table 1.

2.7. Sequence alignments and phylogenetic analysis

All protein sequence alignments were made using the program ClustalX (version 1.83) [26]. The sequences were

Table 1
Homologue protein sequences to the BjussuMP-I catalytic domain found at the NCBI and UniProt databases

Protein (four-letter identification code)	Species or subspecies	ID code
Protein sequences from Viperidae family		
Metalloprotease BOJUMET I (Bjus)	*Bothrops jararacussu*	gb|AAP78952.1
Metalloprotease BaP1 (Basp)	*Bothrops asper*	pdb|1ND1
Metalloprotease precursor (Gsax)	*Gloydius saxatilis*	gb|AAP20642.1
Insularinase and insularin precursor (Bins)	*Bothrops insularis*	gb|AAU47334.1
Piscivostatin beta chain (Apis)	*Agkistrodon piscivorus piscivorus*	dbj|BAC55947.1
Metalloprotease (Ghal)	*Gloydius halys*	gb|AAD02655.1
Lebetase isoform Le-4 (Mleb-1)	*Macrovipera lebetina*	gb|AAY45880.1
Non-hemorrhagic fibrin(ogen)olytic metalloprotease (Bneu)	*Bothrops neuwiedi*	gb|AAF28364.1
Jararhagin (Bjar)	*Bothrops jararaca*	emb|CAA48323.1
Hemorrhagic metalloprotease HR1b (Tfla-1)	*Trimeresurus flavoviridis*	dbj|BAB92014.1
Adamalysin II (Cada)	*Crotalus adamanteus*	pdb|1IAG
Metalloprotease 4 (Bgab)	*Bitis gabonica*	gb|AAR19273.1
Metalloprotease atrolysin E (Catr)	*Crotalus atrox*	gb|AAB23201.1
Stejnihagin-A (Vste-1)	*Viridovipera stejnegeri*	gb|ABA40760.1
Acutolysin A (Dacu-1)	*Deinagkistrodon acutus*	gb|AAD51824.1
Berythractivase (Bery)	*Bothrops erythromelas*	gb|AAL47169.1
Stejnihagin-B (Vste-2)	*Viridovipera stejnegeri*	gb|ABA40759.1
Metalloprotease (Epyr)	*Echis pyramidum*	emb|CAA55566.1
Trimutase precursor (Pmuc)	*Protobothrops mucrosquamatus*	gb|AAB94016.1
Zinc metalloprotease flavoridin precursor (Tfla-2)	*Trimeresurus flavoviridis*	sp|P18619
Prothrombin activator EoMP06 (Eoce)	*Echis ocellatus*	gb|AAP92424.1
Acutolysin C (Aacu)	*Agkistrodon acutus*	sp|P60244
Coagulation factor X activating enzyme heavy chain (Vrus)	*Vipera russelli*	gb|AAB22477.1
Aculysin-1 (Dacu-2)	*Deinagkistrodon acutus*	emb|CAB46429.1
Metalloprotease precursor (Cmol)	*Crotalus molossus molossus*	UniProt/TrEMBL|Q8JJ51
Hemorrhagic factor II (Lmut)	*Lachesis muta muta*	UniProt|P22796
Metalloprotease precursor (Acon)	*Agkistrodon contortrix*	gb|AAC59703
Fibrolase (Mleb-2)	*Macrovipera lebetina*	sp|P83255
Protein sequences from Elapidae family		
Mocarhagin 1 (Nmos)	*Naja mossambica mossambica*	gb|AAM51550.1
Hemorrhagic metalloprotease kaouthiagin (Nkao)	*Naja kaouthia*	UniProt/Swiss-Prot|P82942
Cobrin precursor (Nnaj)	*Naja naja*	UniProt/TrEMBL|Q9PVK7
Metalloprotease precursor (Amic-1)	*Atractaspis microlepidota andersoni*	gb|AAF01040.1
Metalloprotease precursor (Amic-2)	*Atractaspis microlepidota andersoni*	gb|AAF01041.1
Other related protein sequences		
ADAM metallopeptidase domain 28 (Ggal-1)	*Gallus gallus*	ref|NP_001026058.1
Protein similar to ADAM 13 (Ggal-2)	*Gallus gallus*	ref|XP_420886.1
ADAM metallopeptidase domain 9 (Ggal-3)	*Gallus gallus*	ref|NP_001026567.1
Protein similar to a disintegrin and metalloprotease domain 21 preproprotein (Ggal-4)	*Gallus gallus*	ref|XP_428276.1
Disintegrin and metalloprotease domain 28 isoform 1 (Mmus-1)	*Mus musculus*	ref|NP_034212.1
Disintegrin and metalloprotease domain 8 (Mmus-2)	*Mus musculus*	ref|NP_031429.1
Unnamed protein product (Mmus-3)	*Mus musculus*	dbj|BAE27990.1
Disintegrin and metalloprotease domain 7 (Mmus-4)	*Mus musculus*	ref|NP_031428.1
ADAM metallopeptidase domain 12 isoform 2 preproprotein (Hsap-1)	*Homo sapiens*	gb|AAH60804.1
Metalloprotease-disintegrin meltrin beta (Hsap-2)	*Homo sapiens*	gb|AAG50282.1
ADAM metallopeptidase domain 8 precursor (Hsap-3)	*Homo sapiens*	ref|NP_001100.2
ADAM metallopeptidase domain 28 isoform 1 preproprotein (Hsap-4)	*Homo sapiens*	ref|NP_055080.1
Disintegrin and metalloprotease domain 7 (Hsap-5)	*Homo sapiens*	ref|NP_003808.1
Unknown protein (Xlae-1)	*Xenopus laevis*	gb|AAH91726.1
ADAM 13 (Xlae-2)	*Xenopus laevis*	gb|AAB51194.1
Metalloprotease-disintegrin (Xlae-3)	*Xenopus laevis*	gb|AAC61846.1
Protein similar to a disintegrin and metalloprotease domain 28 isoform 1 preproprotein (Drer-1)	*Danio rerio*	ref|XP_686264.1
Protein similar to a disintegrin and metalloprotease domain 8 (Drer-2)	*Danio rerio*	ref|XP_684931.1
Disintegrin and metalloprotease domain 8 (Drer-3)	*Danio rerio*	ref|NP_956931.1
SD04095p (Dmel)	*Drosophila melanogaster*	gb|AAO39439.1
Hypothetical protein C04A11.4 (Cele)	*Caenorhabditis elegans*	emb|CAA94147.1

aligned using the PAM series protein weight matrices for the pairwise and multiple alignments, with the default values for gap parameters (open and extension penalties). The phylogenetic and molecular evolutionary analyses were conducted using MEGA version 2.1 [27].

Trees were generated by Neighbor-Joining using the following parameters: complete deletion, Poisson correction, and bootstrap with 2000 replications. The protein sequences utilized in this analysis and their respective four-letter identification codes in the phylogenetic trees are shown in Table 1.

2.8. Protein modeling

All the alignments between the BjussuMP-I catalytic domain sequence and the other homologue molecules deposited in structural databases were generated using the program HHpred [27] available at the Max-Planck Institute for Developmental Biology server (http://protevo.eb.tuebingen.mpg.de/toolkit) and based in a threading method. The structure of BaP1 – a metalloproteinase from *Bothrops asper* snake venom (PDB code 1ND1) [28] – was selected and used as template by the program MODELLER 8v2 [29] to build the initial model of the BjussuMP-I catalytic domain. The Zn^{2+} ion and the structural water molecules present in the template structure were added to the initial model using the program MODELLER 8v2 [29]. The structural models of the mocarhagin 1 from *Naja mossambica mossambica* (Nmos), and unknown protein (Xlae-1) and ADAM 13 (Xlae-2) from *Xenopus laevis* were generated through a threading method using the program Fugue [30] (http://www-cryst.bioc.cam.ac.uk/fugue/prfsearch.html).

2.9. Molecular dynamics simulation

The molecular dynamics (MD) simulation was executed using the GROMACS program (Groningen Machine for Chemical Simulation) package version 3.3.1 [31,32] and explicit water molecules, in a Dual Intel Xeon 64 using a SuSe Linux operational system. The simple point charge (SPC) model was used to represent the water molecules [33]. Protonation states of charged groups in each model were set according to pH 7.0. Counter ions were added to neutralize the system and the GROMOS 96 53a6 force field [34] was chosen to perform the MD simulation. The MD simulation was performed at constant temperature and pressure in a periodic truncated dodecahedron box. The minimum distance between any atom of the protein and the box wall was 1.2 nm.

The following protocol was used to generate the starting configuration for the system: after energy minimization (EM) using a steepest descent algorithm, 200 ps of molecular dynamics with position restraints applied to the protein (PRMD) were performed at 298 K to relax the system gently. Then, an unrestrained MD was executed at 298 K during 5 ns of simulation to assess the stability of the structures. During the simulations, temperature and pressure (1.0 bar) were maintained by the coupling to an external heat and an isotropic pressure bath [35]. The distances between the catalytic histidines and the Zn^{2+} ion were kept according to Andreini et al. [36].

2.10. Evaluation of the theoretical BjussuMP-I catalytic domain model

The overall geometric quality of the final theoretical BjussuMP-I catalytic domain model was checked through the programs PROCHECK v.3.5.4 [37] and ProSa2003 [38]. The structural coordinates of the final theoretical BjussuMP-I catalytic domain model have been deposited in the RCSB Protein Data Bank under accession code 2DX9.

2.11. Identification of conserved surface residues

The identification and localization of the conserved surface residues were executed through the program Chimera [39] and based on the final theoretical BjussuMP-I catalytic model and threading models of the mocarhagin 1 from *Naja mossambica mossambica* (Nmos), and unknown protein (Xlae-1) and ADAM 13 (Xlae-2) from *Xenopus laevis*. The figures of the structural models with the conserved surface residues were generated with the program PyMOL [40].

3. Results and discussion

3.1. Fibrinolytic and platelet aggregation effects of BjussuMP-I

In a previous study we showed that BjussuMP-I degraded the $A\alpha > B\beta$ chain of fibrinogen, classifying it as a α-fibrinogenase [22]. In Fig. 1A direct proteolysis of fibrin clots is observed with BjussuMP-I confirming the fibrin(ogen)olytic mechanism of the enzyme. In order to eliminate a possible indirect effect, we used plasminogen-free fibrinogen. The minimum fibrinolytic dose (MFD) is defined as the dose of enzyme which results in a halo of 10 mm diameter. BjussuMP-I degraded fibrin with MFD ≅ 6.0 μg.

Fibrinogenolytic enzymes are naturally found in Viperidae, Elapidae and Crotalidae snake venoms. As reviewed by Swenson and Markland [41], since 1700 several attempts have been made in order to find a practical application of proteolytic enzymes in blood disorders. With some exceptions, from the 67 fibrin(ogen)olytic enzymes reported, 46 are high or low molecular weight metalloproteases, hemorrhagic or non-hemorrhagic. These enzymes are classified as α and β fibrinogenases in virtue of degrading preferentially (although not exclusively) either α or β chains of fibrinogen, respectively. In addition, most of metalloproteases are both fibrinogenolytic and fibrinolytic enzymes (for more details, see [8,41]).

One of the major medical interests for snake venom proteases may be their use as sources of potential pharmaceutical agents. Indeed, because of their broad spectrum of proteolytic activity leading to fibrinogen and/or fibrin degradation, they can be true anticoagulants or templates to obtain new drugs. Regarding that, in vitro and in vivo studies

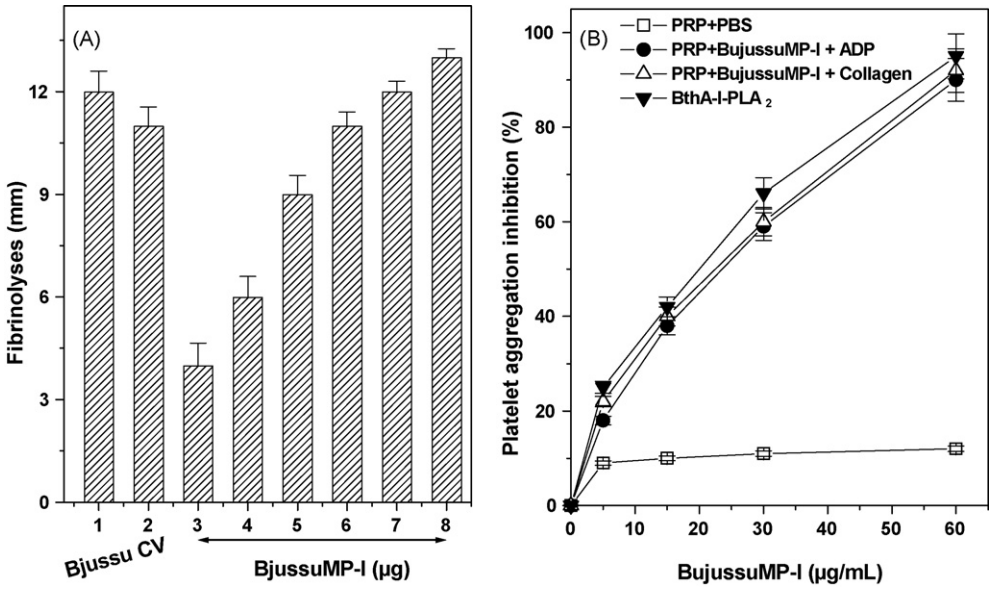

Fig. 1. Effects of BjussuMP-I upon fibrin and platelets. (A) Fibrinolytic activity of BjussuMP-I upon plates containing fibrin clots. (1,2) *Bothrops jararacussu* CV (15.0 μg), (3–8) BjussuMP-I in different concentrations (3.0, 6.0, 15.0, 30.0, 60.0 and 120.0 μg). (B) Inhibition of ADP- and collagen-induced platelet aggregation by BjussuMP-I. Rich plasma platelets suspensions containing 4×10^5 platelets/μL were incubated with different concentrations of BjussuMP-I and for 2 min before adding 2.0 μg/mL ADP or collagen. Results are expressed as percentages of positive and negative control values using acidic PLA_2 (BthA-IPLA$_2$) and PBS, respectively. Each bar represents the mean ± S.D. ($n = 3$).

using hemorrhagic or non-hemorrhagic metaloproteases have been demonstrated that these compounds may have potential application in thrombolytic therapies [42,43].

In order to investigate the effect of BjussuMP-I and to suggest a mechanism involved in platelet modulation (Fig. 1B), we show the aggregation of platelets triggered by ADP and collagen. To compare the effects of BjussuMP-I, we used a *B. jararacussu* acidic phospholipase A_2 (BthA-I-PLA$_2$) as a platelet aggregation inhibitor. In Fig. 1B, we observed that the BjussuMP-I inhibited platelet aggregation triggered by collagen or ADP. Recently, snake venom proteins such as disintegrins and disintegrin-like metalloproteases have been shown to be selective for integrin receptors, providing new insights into molecular mechanisms on platelet adhesion. This fact proves these proteins are useful to identify targets for novel anti-thrombotic or diagnostic reagents [14,44].

3.2. Primary structure of BjussuMP-I: N-terminus and cDNA sequencing

BjussuMP-I was first isolated from *B. jararacussu* by Mazzi et al. [22]. The primary sequence of this protein consists of 546 amino acid residues, with a high percentage of polar groups (Asp, Glu, Gly). As confirmed by the cDNA sequence (Fig. 2), the amino acid composition of BjussuMP-I shows this molecule has a possible acidic character, with a theoretical p$I \cong 5.65$ and $M_r \cong 61930.6$, and also shows the presence of 29 half-cystine residues. In previous studies, Bjarnason and Fox [2] suggested that the high cysteine content and the disintegrin-like domain might be involved in the hemorrhagic effect. BjussuMP-I presented hemorrhage on mouse back skin when micrograms (MHD = 4.5 μg) of enzyme was injected subcutaneously [22]. Recent research has been reported that the domain of P-III class SVMPs has a considerable content of cysteinyl (Cys) residues [19]. Moreover, the Cys residues and the intra-domain disulfide bonds found in variable positions of the P-III metalloproteases, may be associated with the structural stability of the molecule containing disintegrin-like and cysteine-rich residues [19,45].

The identity of the BjussuMP-I cDNA was confirmed by N-terminal amino acid sequence, E-QQKFPYRYVEIVVVD-RRHV, which together with the amino acid sequence of other SVMPs from P-III class, were used to design the primers. The degenerate primers were designed for cDNA amplification and the PCR products analysis revealed a cDNA sequence of 1.6 kb (results not shown).

The sequence search of the GenBank data base revealed that BjussuMP-I has a high sequence identity with other P-III SVMPs. The sequence identities of BjussuMP-I precursor with those snake venom metalloprotease precursors was shown in Fig. 3. The protease, disintegrin, and cysteine-rich domains in mature BjussuMP-I are composed of 207, 100 and 127 amino acid residues, respectively.

According to the deduced amino acid sequence analysis of BjussuMP-I, we found an open reading frame of 547 amino acid residues, consisting of conserved domains of P-II and P-III high molecular weight hemorrhagic metalloproteases. In Fig. 3, we observed a multidomain structure comprised of a proprotein sequence of 133 residues and a mature protein of 414 residues, including a cysteine switch motif, metalloprotease, disintegrin and cysteine-rich domains. BjussuMP-I is a potentially active hemorrhagic and proteolytic protein, which is inhibited by chelating agents [22]. We also identified the sequence of the consensus zinc-binding site (H-E-L-G-H-N-L-G-M-E-H-D) localized in its metalloprotease domain, which is constituted by 218 amino acid residues. The conservative presence of zinc-binding domain histidine residues is essential for both stability

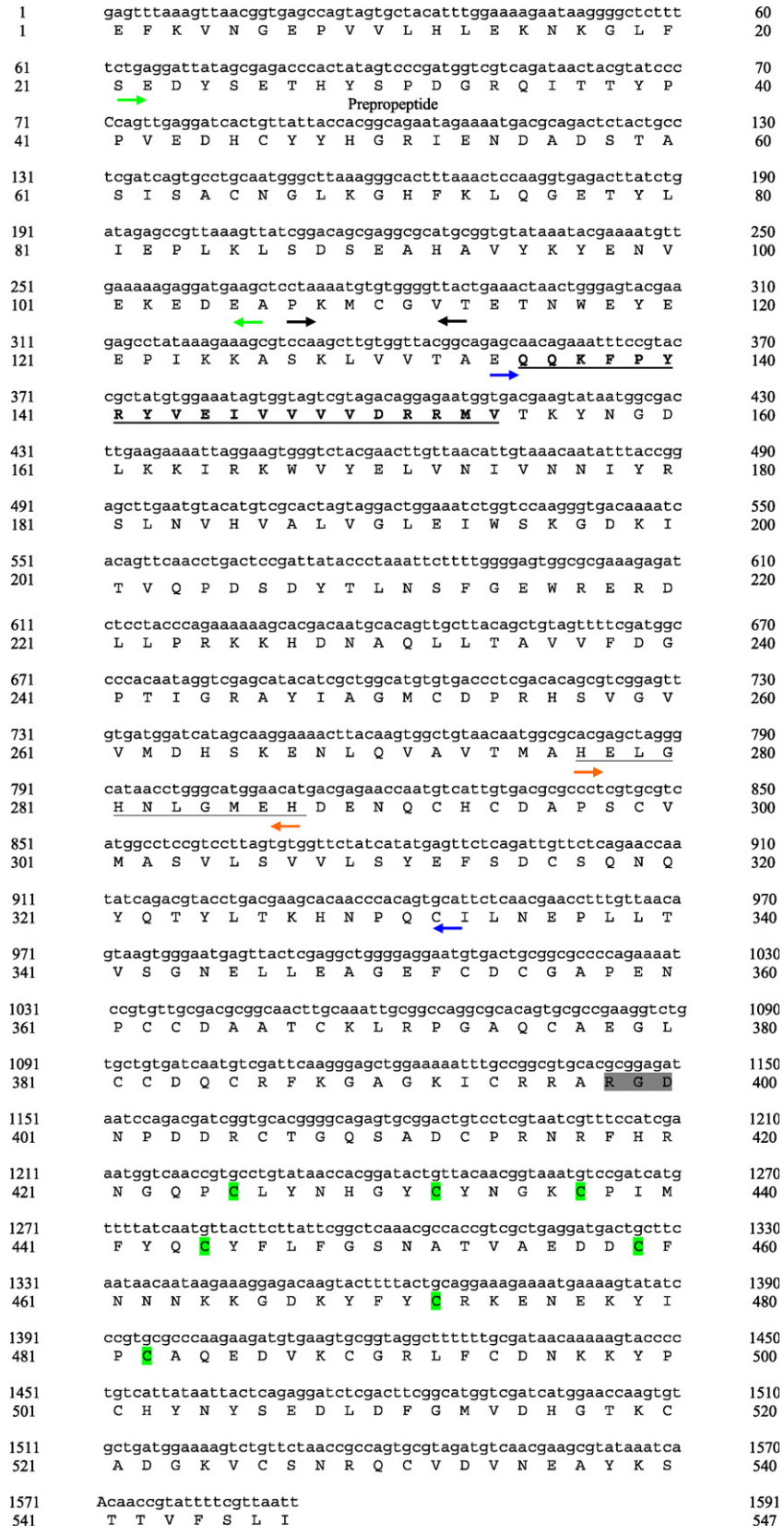

Fig. 2. The cDNA and deduced amino acid sequence of BjussuMP-I. The deduced amino acid sequence is represented by one-letter code, witch the cDNA sequence with 1540 pb encoded open reading frames the follow 547 amino acid residues: pre-pro-peptide, metalloprotease, residues determined by protein sequencer cysteine switch motif (PKMCGVT), a zinc-binding motif (HELGHNLGMEHD) disintegrin-like and a rich cysteine domain.

of the active site and the proteolytic activity of the enzyme [2,22].

Based on molecular characteristics, large SVMPs are also designed as MDC enzymes, due to the presence of structure revealing an N-terminal *metalloprotease* domain, a *d*isintegrin-like domain and a *C*ys-rich C-terminus. According to the primary structures of most MDC enzymes, in spite of having an ECD motif instead of RGD, they share some similar structural and functional properties which enable these proteins to recognize integrin cell surface receptors [46]. More recently, acurhagin, a P-III SVMP purified from *Agkistrodon acutus* venom [47] was reported as a P-III hemorrhagic metalloprotease containing Ser-Glu-Cys-Asp (SECD) sequence in the disintegrin-like domain instead of the typical Arg-Gly-Asp (RGD) or commonly ECD/DCD motifs.

3.3. Phylogenetic analysis of the BjussuMP-I catalytic domain

The phylogenetic analysis of the BjussuMP-I catalytic domain was performed in two parts: (i) the study of the evolutionary origins of the SVMPs and (ii) the search for possible relations between the toxins which were selected to carry through this work.

Initially, a phylogenetic tree was built to determine the evolutionary relations between the SVMPs and the cellular metalloproteases from other organisms, using sequences selected in the NCBI and Pfam databases. As expected, the sequences found in the Pfam database were identified as Reprolysin domains. These catalytic domains are present in animals, fungi and *Bacillus licheniformis* (strain dsm 13) (UniProt/TrEMBL|Q65DR9), a well-known soil bacterium used for biotechnological applications. The presence of this reprolysin sequence in the *B. licheniformis* could be explained by a horizontal genetic transmission occurred between an unknown species of animal or fungi (most probably a soil fungi) and this bacterium. Therefore, taking into account this hypothesis about the origin of the reprolysin sequence in *B. licheniformis*, the first reprolysin domain appeared in the last common ancestor of Metazoa and Fungui.

The sequences found in Fungi and *B. licheniformis* were not included in the phylogenetic analysis due to their low identity degree in relation to the others. Then, the homologue sequence of *C. elegans* was used as root in the first phylogenetic tree (Fig. 4A). This ancestral gene of the metalloproteases is related

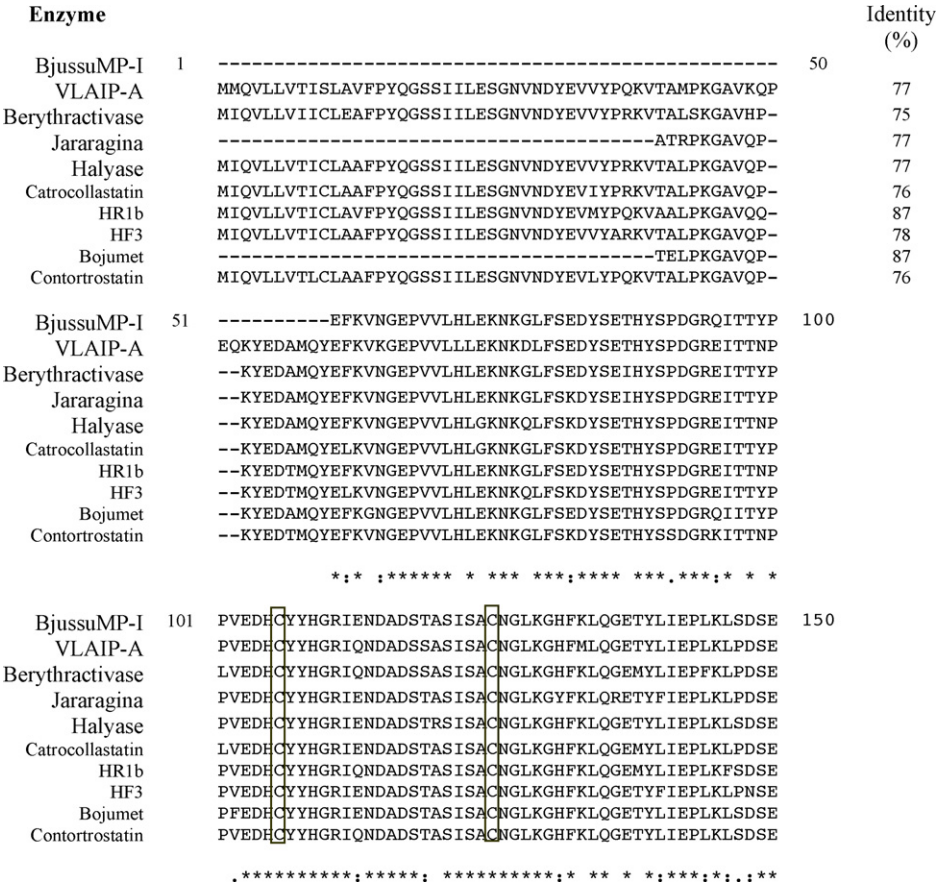

Fig. 3. Comparison of BjussuMP-I multiple sequence with conserved sequences of others SVMPs: By multiple alignment, cysteine residues (boxed) "cys switch", zinc-binding and disintegrin motifs (bold typed). (*) Positions fully conserved; (:) conservative variation/exchange of a amino acid; (·) non-conservative variation/exchange of a amino acid. The aa sequences of BjussuMP-I were aligned with: VLAIP-A from *M. Lebetina* (gi: 61104775), Berythractivase from *B. erytromela* (gi: 17865171), Jararagin from *B. jararaca* (gi: 62468), Halyase from *G. halys* (gi: 607296954), Catrocollastatin from *C. atrox* (gi: 710354), HR1b from *T. flavoviridis* (gi: BAB92014), HF3 from *B. jararaca* (gi: 31742525), Bojumet from *B. jararacussu* (gi: 32306929) and Contortrostatin from *Agkistrodon contortrix* (gi: 7630286).

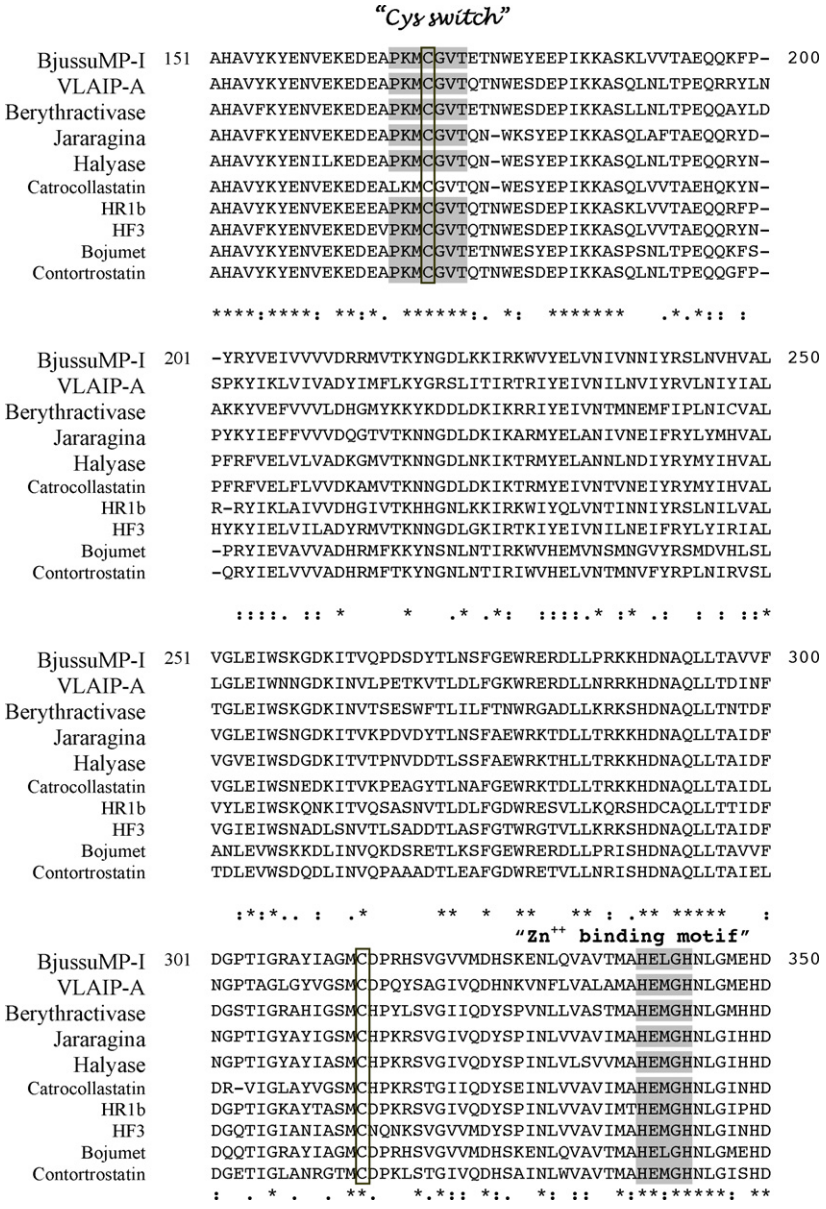

Fig. 3. (*Continued*)

to the gonad morphogenesis and cell adhesion in *C. elegans* [48,49]. In the main branch, there is an unequivocal relation between the SVMPs and others identified in different species (Drer-1, Xlae-1, Ggal-1, Mmus-1, Mmus-4, Hsap-4, and Hsap-5). Thus, despite all metalloproteases selected here are taking part in the reprolysin family, some molecules from *Xenopus laevis*, *Danio rerio*, *Gallus gallus*, *Mus musculus*, and *Homo sapiens* are more related to the SVMPs than others. Based on this information, it was possible to classify the sequences in four groups (viperid SVMPs, elapid SVMPs, proto-SVMPs, and non-SVMPs), according to their phylogeny and phenotype (Fig. 4A). The sequences from Drer-1, Xlae-1, Ggal-1, Mmus-1, Mmus-4, Hsap-4, and Hsap-5 were classified as proto-SVMPs due to their phylogenetic relation with the SVMPs, since these sequences are in a monophiletic branch. The analysis of the phylogenetic tree shows that the evolutionary history of the proto-SVMPs began with a primitive gene duplication which occurred before the emergence of the common ancestor of teleosts and tetrapods. Also is possible to conclude that new and independent duplication events occurred in mammals, birds, and teleosts, whereas it was not possible to find in the databases more than one reprolysin isoform in the snake species. However, the lack of a complete snake genome sequence does not allow us to conclude whether reprolysin isoforms are not present in these animals. Therefore, it is possible to suppose that mutations in a proto-SVMP of a snake ancestor can be responsible by the transformation of these domains with an endogenous function in a potent toxin, even though the lack of homologue sequences in other reptiles could be an obstacle for this hypothesis.

The second part of this phylogenetic analysis was executed with the catalytic domain sequences of all SVMPs selected in the NCBI and UniProt databases (Fig. 4B). As shown in the phylogenetic tree (Fig. 4B), it was not possible to arrange these

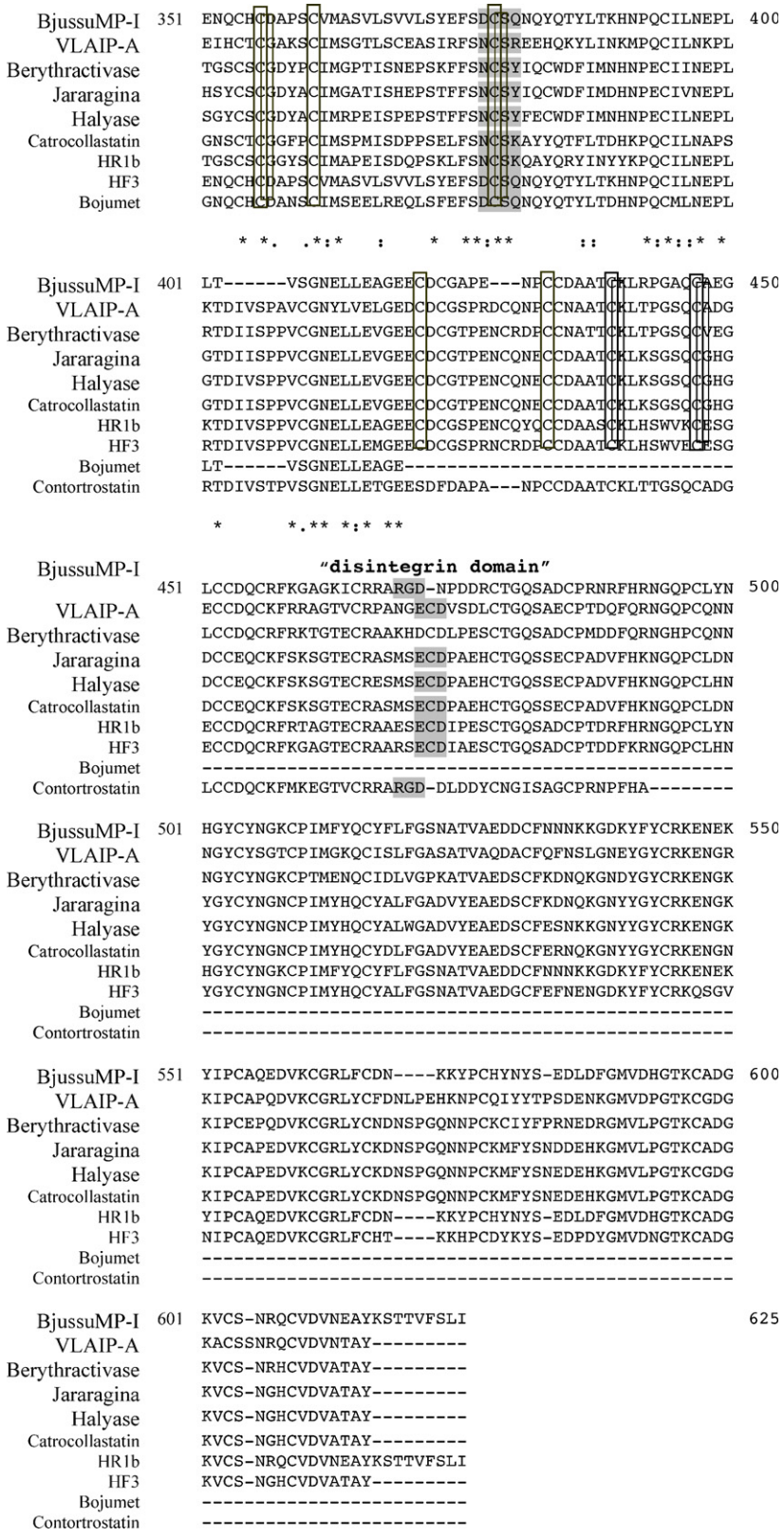

Fig. 3. (*Continued*).

metalloproteases in separated branches according to their capacity of inducing hemorrhage. Similarly, these results were also obtained by Ramos and Selistre-de-Araújo [21]. Analyzing this tree is also possible to suggest that the hemorrhagic activity was a biochemical activity present in the first SVMPs due to the higher number of hemorrhagic toxin sequences obtained in the databases. Apparently, some of these toxins lost this activity during the process of molecular evolution of the SVMPs. The

reasons for the lack of hemorrhagic action are not clear and could be related to new roles played by these non-hemorrhagic SVMPs. Furthermore, a more detailed analysis of this phylogenetic tree shows a remarkable separation between the Viperidae family species and those from other groups. The sequences from *Atractaspis microlepidota* (Amic-1 and Amic-2) (Atractaspididae family), and those from *Naja kaouthia* (Nkao), *Naja naja* (Nnaj) and *Naja mossambica mossambica* (Nmos) (Elapidae family) were grouped in a separated branch. This phylogenetic separation suggests that the SVMPs from Viperidae, Elapidae, and Atractaspididae families could present distinct biochemical functions and/or different pharmacological activity degrees. The high degree of evolutionary pressure involved in the molecular evolution of venom toxins supports this hypothesis. It is also important to emphasize the second part of the phylogenetic analysis was only performed with

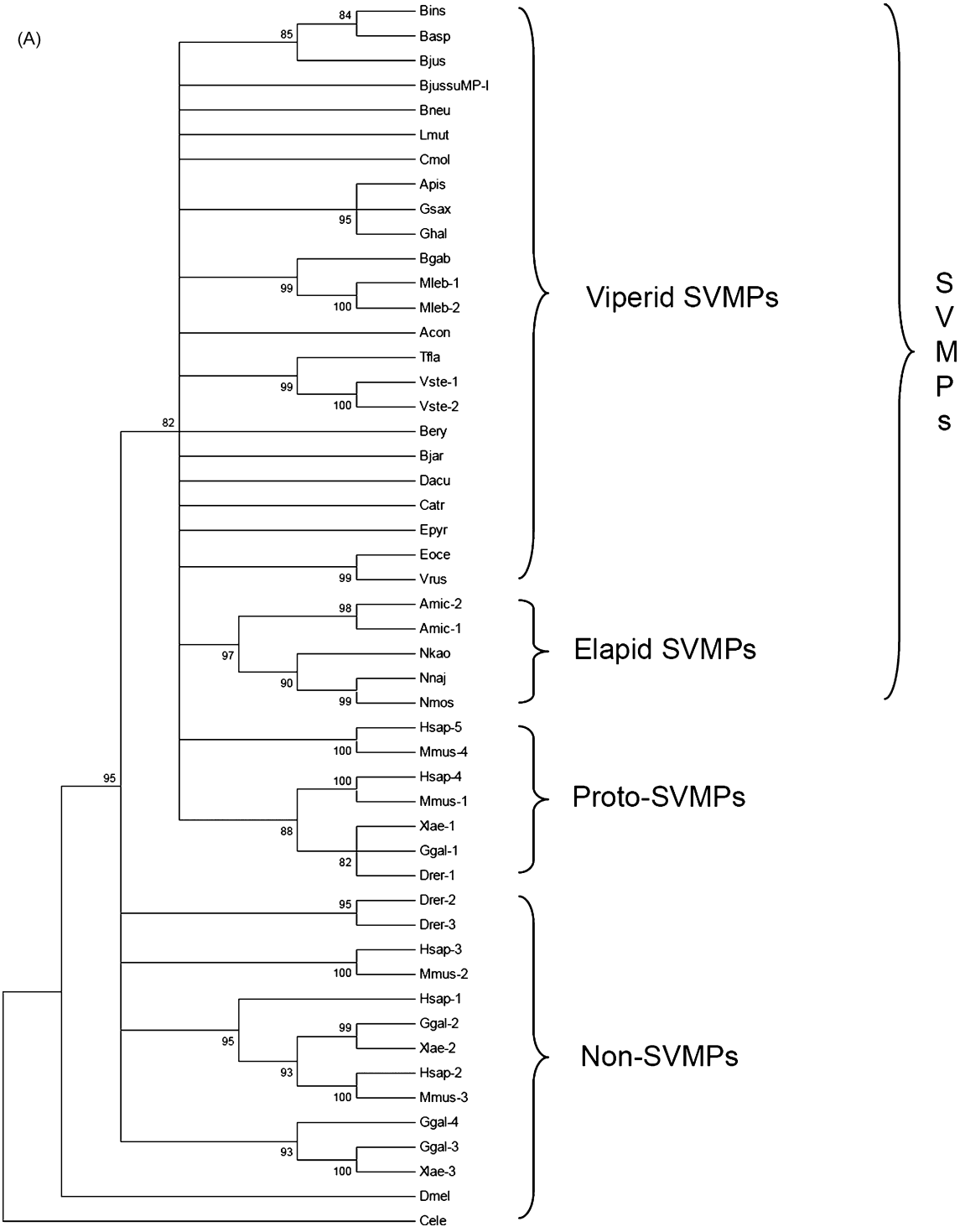

Fig. 4. Phylogenetic analysis. Phylogenetic tree built with sequences of metalloproteases (A) and SVMPs (B) selected in the databases. The bootstrap values are shown in the branches. Generated by the program Mega [26]. In (B) the hemorrhagic metalloproteases are labeled with asterisks.

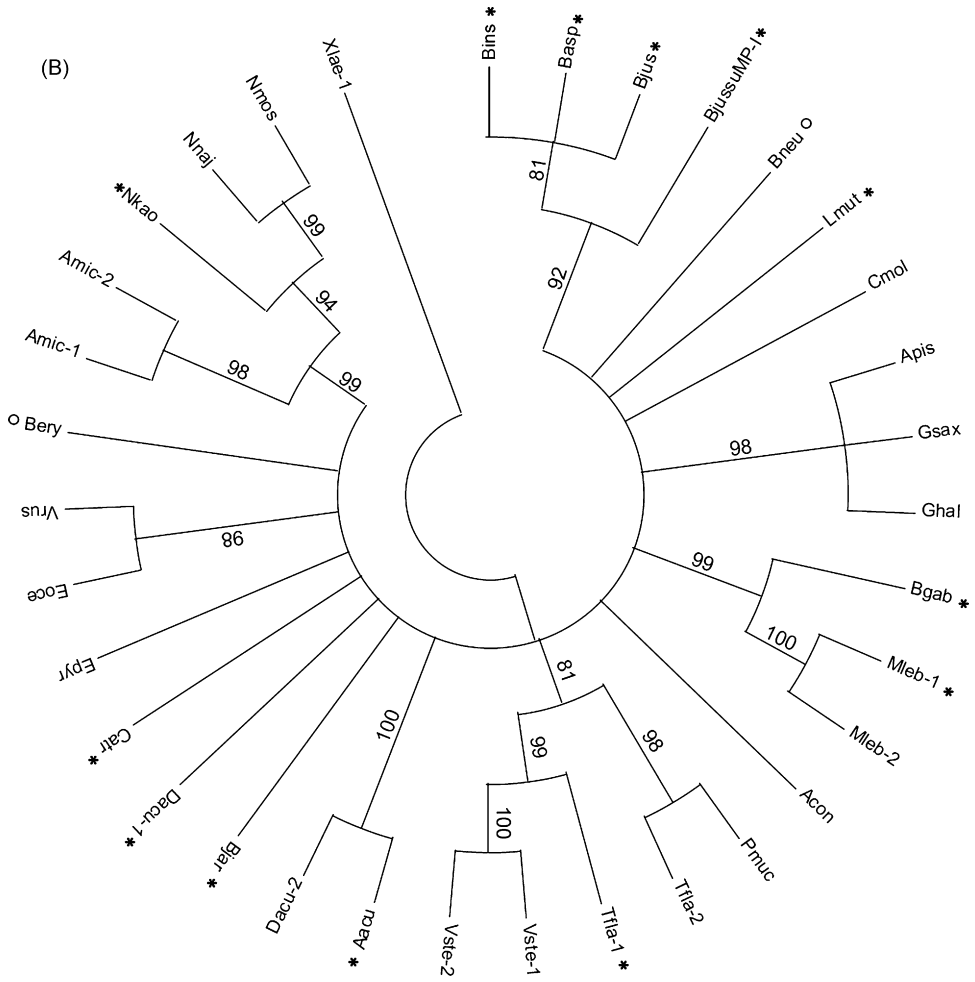

Fig. 4. (*Continued*).

catalytic domain sequences obtained from SVMPs. Therefore, the other domains from these toxins may present variations still more significant in relation to the nature of their biochemical and pharmacological activities.

Finally, the SVMPs and some corresponding molecules present in other organisms have a close evolutionary relation. This connection makes these toxins good models for the investigation of adhesion, cell fusion, intracellular signaling and reproductive roles played by the metalloproteases in the metabolic pathways and physiology of different species, mainly in humans and other mammals.

3.4. BjussuMP-I catalytic domain theoretical model: modeling, molecular dynamics simulation and structural analysis

Initially, the primary sequence of the BjussuMP-I catalytic domain was utilized to build several alignments [27] based on a threading method of several homologue proteins deposited in structural databases. The structure of BaP1 (metalloproteinase from *Bothrops asper*) [28] was selected due to its identity degree with the BjussuMP-I catalytic domain sequence (71%) and in the score (442.93) attributed by the program HHpred [27] to the alignment of these two sequences. BaP1 structure was used as template to build the initial model of the BjussuMP-I catalytic domain [29]. R.M.S.D. of the BjussuMP-I catalytic domain model was stabilized around 1500 ps during the molecular dynamics simulation (Fig. 5A). After the stabilization point, the atoms of the model suffered a slight variation in their positions of approximately 0.1 nm, which indicates the final model is stable and probably consistent. The Ramachandran plot [37] (Fig. 5B) shows 98.3% of the model residues are in the core and additionally allowed regions. Furthermore, the graph calculated by the program ProSa2003 [38] shows all residues have negative potential energies indicating the high stability degree of the model (Fig. 5C). Thus, all these results demonstrate the BjussuMP-I catalytic domain theoretical model is feasible.

The final model is very similar to other three-dimensional BjussuMP-I catalytic domains already described [25,50–52], presenting an ellipsoidal form and two subdomains. The major subdomain is constituted by the first 152 residues and presents four α-helices (h1, h2, h3, and h4) and six stranded β-sheets (β_1, β_2, β_3, β_4, β_5, and β_6), while the last 98 residues belong to the minor subdomain, which is formed by one α-helix and several loops (Fig. 6A). However, the catalytic histidines show

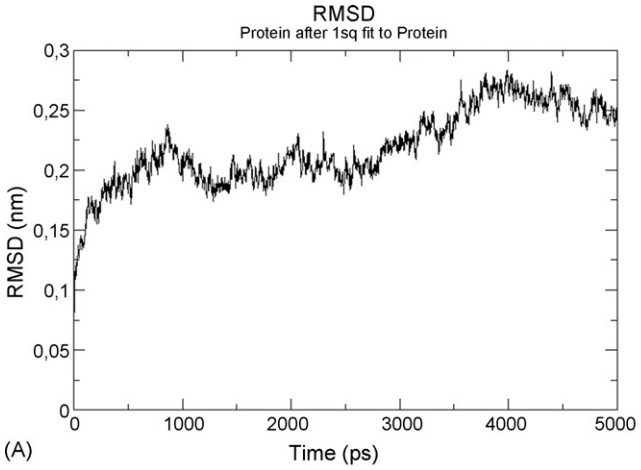

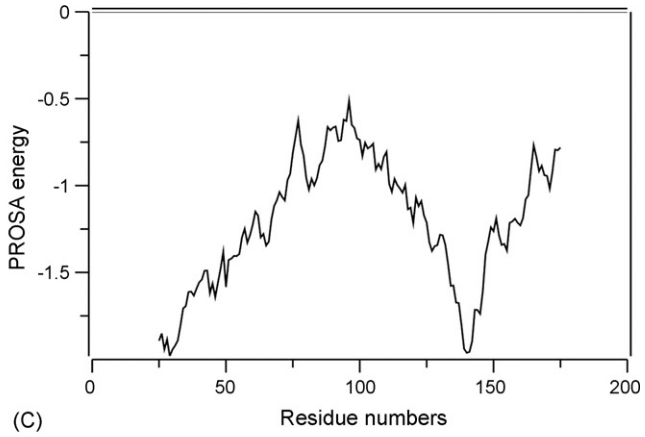

PROCHECK

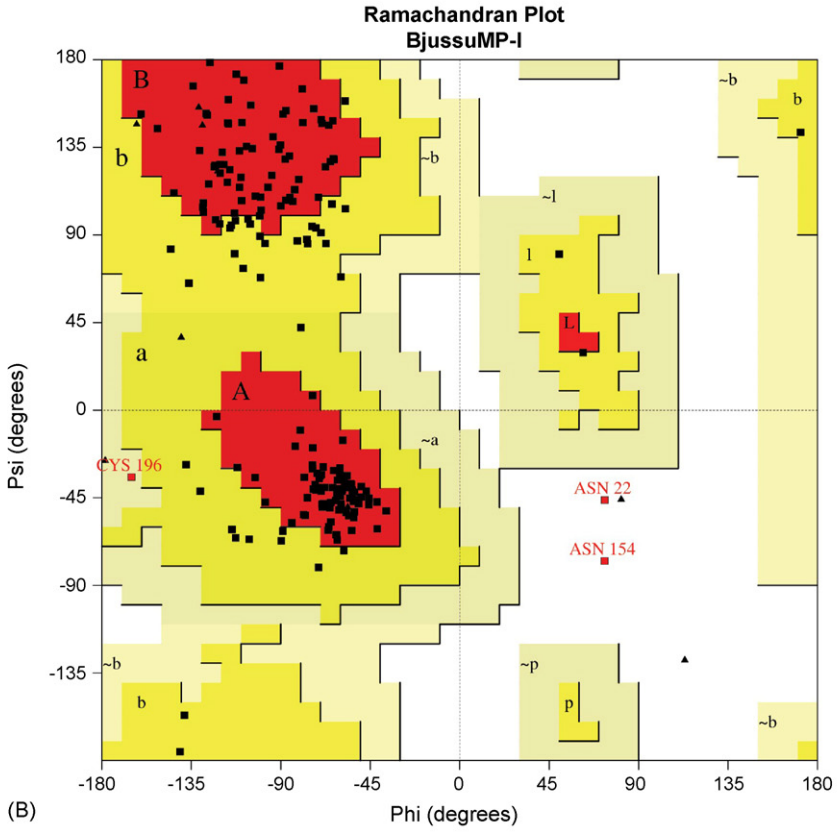

Plot statistics

Residues in most favoured regions [A,B,L]	140	77.3%
Residues in additional allowed regions [a,b,l,p]	38	21.0%
Residues in generously allowed regions [~a,~b,~l,~p]	1	0.6%
Residues in disallowed regions	2	1.1%
Number of non-glycine and non-proline residues	181	100.0%
Number of end-residues (excl. Gly and Pro)	3	
Number of glycine residues (shown as triangles)	10	
Number of proline residues	7	
Total number of residues	201	

Based on an analysis of 118 structures of resolution of at least 2.0 Angstroms and R-factor no greater than 20%, a good quality model would be expected to have over 90% in the most favoured regions.

Fig. 5. Molecular dynamics. (A) BjussuMP-I catalytic domain R.M.S.D. deviation during the molecular dynamics (MD) simulation. The stabilization of the structure occurred approximately in 500 ps. Generated by GROMACS [31]. (B) Ramachandran plot. Generated by the program PROCHECK v.3.5.4 [37]. (C) ProSa energy profile. Generated with the program Prosa [38].

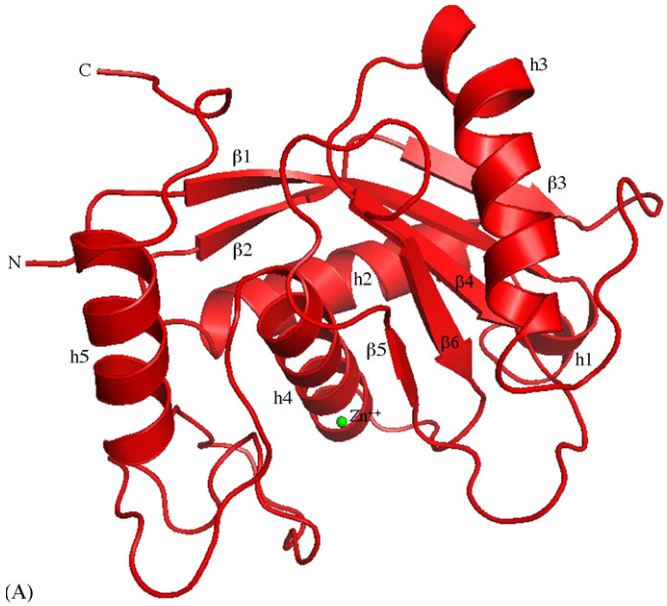

(A)

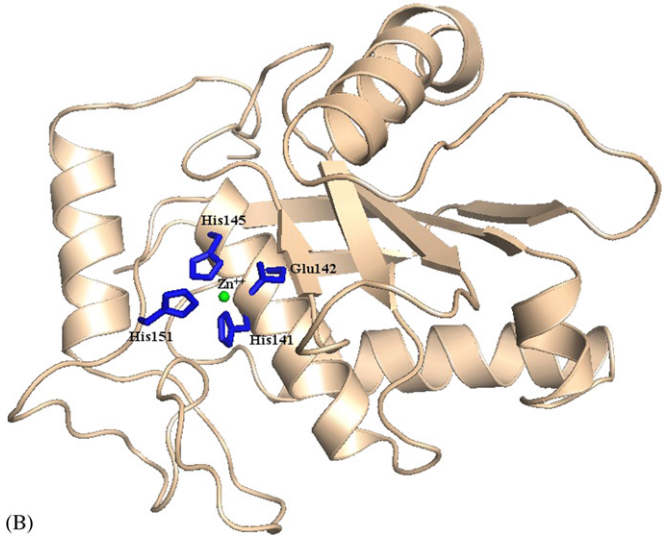

(B)

Fig. 6. Structure of BjussuMP-I. (A) Secondary and tertiary structure of the final theoretical BjussuMP-I catalytic domain model. The ion Zn^{2+} is shown as a green sphere. Generated by the program PyMOL [40]. (B) Final theoretical BjussuMP-I catalytic domain model showing the side chains of the catalytic histidines as blue sticks. The ion Zn^{2+} is shown as in (A). Generated by the program PyMOL [40].

a good structural relation: His141 and His145 from h4 and His151 from the Met-turn (a conserved motif present in zinc-peptidases [53]) keep their imidazole rings in a favorable position to coordinate the catalytic zinc (Fig. 6B).

Structure–function relationships of some P-I metalloproteases have been identified in recent works [21,52]. These studies indicate that the differentiation between the hemorrhagic and non-hemorrhagic P-I metalloproteases can only be deduced by structural comparison. On this basis, the structural comparison between the theoretical catalytic domain of the BjussuMP-I, a P-III metalloprotease, and the other sequences selected in the databases was realized to understand the evolution of these molecules and to obtain hints about their biochemical activities. The program Chimera [39] was used to

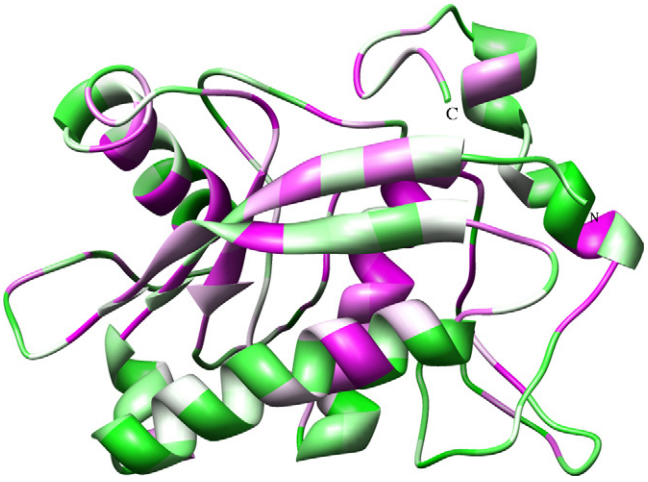

Fig. 7. Ribbon representation of the final theoretical BjussuMP-I catalytic domain model showing the conservation degree between the residues of all sequences of metalloproteases selected in the databases. The regions more conserved are shown in magenta and those with a lower conservation are green. Generated with the program Chimera [39].

identify conserved residues of these molecules in the generated multiple sequence alignments, showing positions of these residues at the three-dimension structure of the sequences used. The analysis of the alignment of all metalloprotease catalytic domain sequences [39] showed few surface residues were conserved during the evolution, in contrast with the internal residues which remained practically unaltered (Fig. 7).

Additionally, the catalytic domain sequences from viperid and elapid SVMPs and other homologue sequences were separated in four groups according to phylogeny and phenotype (see phylogenetic analysis) and aligned separately. The final theoretical BjussuMP-I catalytic domain model and the threading models built with the sequences of the mocarhagin 1 from *Naja mossambica mossambica* (Nmos) and two proteins from *Xenopus laevis* (an unknown protein (Xlae-1) and ADAM 13 (Xlae-2)) were compared using the program Chimera in order to identify the conserved residues present in these four specific alignments. An interesting feature was then revealed about the catalytic domain of the metalloproteases: each group presented a determined set of surface conserved residues. All sets are composed by surface conserved residues present in all sequences. However, there are additional surface conserved residues specifically found in each group. A common characteristic of the molecular surfaces of all metalloproteases aligned, which was not changed during the evolution history of these proteins, is the presence of large hydrophobic areas (data not shown). The independent degree of conservation of these hydrophobic areas suggests that this biochemical architecture was an important factor in the adaptation of the cellular metalloproteases as toxins. It is likely the apolar surfaces present in the substrates of the primitive intracellular metalloproteases keep a high similarity with the proteins attacked by these toxins, particularly in the case of the hemorrhagic SVMPs. However, the most remarkable structural difference between the catalytic domains of the metalloproteases seems to be related to the type and number of the specific

Table 2
Specific conserved surface residues present in the groups of metalloproteases

	SVMPs			
	Viperid SVMPs	Elapid SVMPs	Proto-SVMPs	Non-SVMPs
Specific conserved surface residues	14	56	13	14
Specific positive-charged conserved surface residues	2	8	5	1
Specific negative-charged conserved surface residues	–	5	2	2

Results obtained by the program Chimera [39].

electrostatically charged surface residues present in each group (Table 2 and Fig. 8). This fact shows these charged surface residues may play an important role in the specific biochemical reactions executed by each group of metalloproteases.

Another interesting structural feature that could be a hint to explain the different biological roles of the SVMP catalytic domains and their more related sequences (proto-SVMPs) is found in the positions 15 and 21. In the viperid SVMP catalytic domains, these positions are occupied by positive-charged surface conserved residues (Arg15 or His15 and Lys20), whereas in the proto-SVMPs these positions are occupied only by non-charged residues (Ala15 and Phe20). The elapid SVMPs sequences also present a clear predominance of positive-charged residues at these same positions. Thus, these positive-charged residues may be essential for the biochemical functions played only by the SVMPs.

In conclusion, interesting structural features were identified for the SVMPs and their more related metalloproteases: these molecules are characterized by the presence of large hydrophobic areas and group-specific charged conserved residues (mainly positive-charged residues) at their surfaces. Therefore, these characteristics are probably important for the interaction between these toxins and their substrates. Site-specific mutagenesis and expression experiments with the replacement of the group-specific surface residues conserved in these proteins could help to confirm this theory.

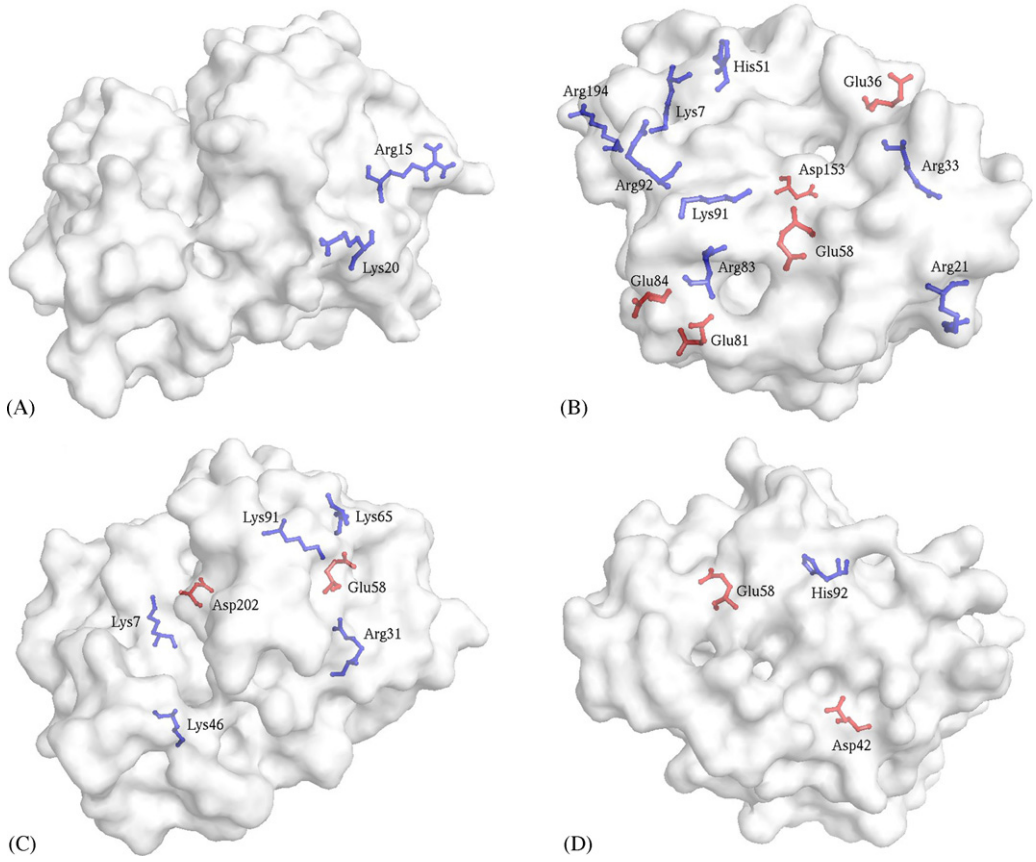

Fig. 8. Specific surface charged residues of the catalytic domains from the metalloproteases classified as viperid SVMPs, elapid SVMPs, proto-SVMPs, and non-SVMPs (respectively labeled as A, B, C, and D). The structures used for the identification (residue number) and localization of the conserved surface residues were the final theoretical BjussuMP-I catalytic domain model (viperid SVMPs), and threading models of the mocarhagin 1 from *Naja mossambica mossambica* (Nmos) (elapid SVMPs) and two sequences from *Xenopus laevis* (an unknown protein (Xlae-1) (proto-SVMPs) and ADAM 13 (Xlae-2) (non-SVMPs)). The positive and negative charged residues are shown, respectively, as blue and red sticks. The conserved residues were identified with the program Chimera [39] and the figures were generated with PyMOL [40].

Acknowledgements

The authors express their gratitude to the Fundação de Amparo à Pesquisa do Estado de São Paulo (FAPESP) and to the Conselho Nacional de Desenvolvimento Científico e Tecnológico (CNPq) for the financial support. We are grateful to Danilo Menaldo (TT-USP) for his helpful technical collaboration.

References

[1] T. Matsui, Y. Fujimura, K. Titani, Snake venom proteases affecting hemostasis and thrombosis, Biochim. Biophys. Acta 1477 (2000) 146–156.
[2] J.B. Bjarnason, J.W. Fox, Hemorrhagic metalloproteinases from snake venoms, Pharm. Ther. 62 (1994) 325–372.
[3] J.M. Gutiérrez, A. Rucavado, Snake venom metalloproteinases: their role in the pathogenesis of local tissue damage, Biochimie 82 (2000) 841–850.
[4] C.A. Silva, J.P. Zuliani, M.T. Assakura, R. Mentele, A.C.M. Camargo, C.F.P. Teixeira, S.M.T. Serrano, Activation of $\alpha_M\beta_2$-mediated phagocytosis by HF3, a P-III class metalloproteinase isolated from the venom of *Bothrops jararaca*, Biochem. Biophys. Res. Commun. 322 (2004) 950–956.
[5] J.M. Gutiérrez, A. Rucavado, T. Escalante, C. Díaz, Hemorrhage induced by snake venom metalloproteinases: biochemical and biophysical mechanisms involved in microvessel damage, Toxicon 45 (2005) 997–1077.
[6] C. Ouyang, C.M. Teng, T.F. Huang, Characterization of snake venom components acting on blood coagulation and platelet function, Toxicon 30 (1992) 945–966.
[7] A.S. Kamiguti, C.R.M. Hay, R.D.G. Theakston, M. Zuzel, Insights into mechanism of haemorrhage caused by snake venom metalloproteinases, Toxicon 34 (1996) 627–642.
[8] F.S. Markland, Snake venoms and the hemostatic systems, Toxicon 36 (1998) 149–180.
[9] I.M.B. Francischetti, H.C. Castro, R.B. Zingali, C.R. Carlini, J.A. Guimarães, *Bothrops* sp. Snake venoms: comparison of some biochemical and physicochemical properties and interference in platelet functions, Comp. Biochem. Physiol. 119 (1998) 21–29.
[10] J. White, Snake venoms and coagulopathy, Toxicon 45 (2005) 951–967.
[11] N. Marsh, V. Willians, Practical applications of snake venom toxins in haemostasis, Toxicon 45 (2005) 1171–1181.
[12] R.K. Andrews, M.C. Berndt, Snake venom modulators of platelet adhesion receptors and their ligants, Toxicon 38 (2000) 775–791.
[13] R.K. Andrews, A.S. Kamiguti, O. Berlanga, M. Leduc, R.D.G. Theakston, S.P. Watson, The use of snake venom toxins as tools to study platelet receptors for collagen and von Willebrand factor, Haemostasis 31 (2001) 155–172.
[14] L.C. Wijeyewickrema, M.C. Berndt, R.K. Andrews, Snake venom probes of platelet adhesion receptors and their ligants, Toxicon 45 (2005) 1051–1060.
[15] K. Trummal, K. Tõnismägi, E. Siigur, A. Aaspõllu, A. Lopp, T. Sillat, R. Saat, L. Kasak, I. Tammiste, P. Kogerman, N. Kalkkinen, J. Siigur, A novel metalloprotease from *Vipera lebetina* venom induces human endothelial cell apoptosis, Toxicon 46 (2005) 46–61.
[16] M.J. Paine, H.P. Desmond, R.D.G. Theakston, J.M. Crampton, Purification, cloning and molecular characterization of a high molecular weight hemorrhagic metalloproteinase, jararagin from *Bothrops jararaca* venom. Insights into the disintegrin gene family, J. Biol. Chem. 267 (1992) 22869–22876.
[17] A.S. Kamiguti, F.S. Markland, Q. Zhou, R.D.G. Theakston, M. Zuzel, Proteolytic cleavage of the β1 subunit of platelet α2β1 integrin by the metalloproteinase jararhagin compromises collagen-stimulated phosphorylation of $pp72^{syk}$, J. Biol. Chem. 272 (1997) 32599–32605.
[18] A.S. Kamiguti, A.M. Moura-da-Silva, G.D. Laing, T. Knapp, M. Zuzel, J.M. Crampton, R.D.G. Theakston, Collagen-induced secretion-dependent phase of platelet aggregation is inhibited by snake venom metalloproteinase jararhagin, Biochim. Biophys. Acta 1335 (1997) 209–217.
[19] W.J. Fox, S.M.T. Serrano, Structural considerations of the snake venom metalloproteinases, key members of the M 12 reprolysin family of metalloproteinases, Toxicon 45 (2005) 969–985.
[20] M.R. Cominetti, J.U. Ribeiro, J.W. Fox, H.S. Selistre-de-Araújo, BaG, a new dimeric metalloproteinase/disintegrin from *Bothrops alternatus* that interacts with $\alpha_5\beta_1$ integrin, Arch. Biochem. Biophys. 416 (2003) 171–179.
[21] O.H.P. Ramos, H.S. Selistre-de-Araujo, Comparative analysis of the catalytic domain of hemorrhagic and non-hemorrhagic snake venom metallopeptidases using bioinformatic tools, Toxicon 44 (2004) 529–538.
[22] M.V. Mazzi, S. Marcussi, G.B. Carlos, R.G. Stabeli, J.J. Franco, F.K. Ticli, A.C. Cintra, S.C. Franca, A.M. Soares, S.V. Sampaio, A new hemorrhagic metalloprotease from *Bothrops jararacussu* snake venom: isolation and biochemical characterization, Toxicon 44 (2004) 215–223.
[23] S.H. Andrião-Escarso, A.M. Soares, M.R.M. Fontes, A.L. Fuly, F.M. Correa, J.C. Rosa, L.J. Greene, J.R. Giglio, Structural and functional characterization of an acidic platelet aggregation inhibitor and hypotensive phospholipase A_2 from *Bothrops jararacussu* snake venom, Biochem. Pharmacol. 64 (2002) 723–732.
[24] D.P.S. Leitão, A.C.M. Polizello, Z. Rothschild, Coagulation and fibrinolysis in capybara (*Hydrochaeris hydrochaeris*), a close relative of guinea-pig (*Cavia porcellus*), Comp. Biochem. Physiol. 125A (2000) 113–120.
[25] J.D. Thompson, T.J. Gibson, F. Plewniak, F. Jeanmougin, D.G. Higgins, The ClustalX windows interface: flexible strategies for multiple sequence alignment aided by quality analysis tools, Nucl. Acids Res. 24 (1997) 4876–4882.
[26] S. Kumar, K. Tamura, I.B. Jakobsen, M. Nei, MEGA2: molecular evolutionary genetics analysis software, Bioinformatics 17 (2001) 1244–1245.
[27] J. Söding, A. Biegert, A.N. Lupas, The HHpred interactive server for protein homology detection and structure prediction, Nucl. Acids Res. 33 (2005) 244–248.
[28] L. Watanabe, J.D. Shannon, R.H. Valente, A. Rucavado, A. Alape-Giron, A.S. Kamiguti, R.D. Theakston, J.W. Fox, J.M. Gutierrez, R.K. Arni, Amino acid sequence and crystal structure of BaP1, a metalloproteinase from *Bothrops asper* snake venom that exerts multiple tissue-damaging activities, Protein Sci. 12 (2003) 2273–2281.
[29] M.A. Marti-Renom, A. Stuart, A. Fiser, R. Sánchez, F. Melo, A. Sali, Comparative protein structure modeling of genes and genomes, Annu. Rev. Biophys. Biomol. Struct. 29 (2000) 291–325.
[30] J. Shi, T.L. Blundell, K. Mizuguchi, FUGUE: sequence-structure homology recognition using environment-specific substitution tables and structure-dependent gap penalties, J. Mol. Biol. 310 (2001) 243–257.
[31] H.J.C. Berendsen, D. van der Spoel, R. van Drunen, GROMACS: a message-passing parallel molecular dynamics implementation, Comp. Phys. Commun. 91 (1995) 43–56.
[32] E. Lindahl, B. Hess, R. van der Spoel, GROMACS 3.0: a package for molecular simulation and trajectory analysis, J. Mol. Mod. 7 (2001) 306–317.
[33] H.J.C. Berendsen, J.P.M. Postma, W.F. van Gunsteren, J. Hermans, Interaction models for water in relation to protein hydration, in: B. Pullman (Ed.), Intermolecular Forces, D. Reidel Publishing Company, Dordrecht, 1981, pp. 331–342.
[34] C. Oostenbrink, T.A. Soares, N.F.A. van der Vegt, W.F. van Gunsteren, Validation of the 53A6 GROMOS force field, Eur. Biophys. J. 34 (2005) 273–284.
[35] H.J.C. Berendsen, J.P.M. Postma, A. DiNola, J.R. Haak, Molecular dynamics with coupling to an external bath, J. Chem. Phys. 81 (1984) 3684–3690.
[36] C. Andreini, L. Banci, I. Bertini, S. Elmi, A. Rosato, Comparative analysis of the ADAM and ADAMTS families, J. Prot. Res. 4 (2005) 881–888.
[37] R.A. Laskowski, M.W. MacArthur, D.S. Moss, J.M. Thornton, PROCHECK: a program to check the stereochemical quality of protein structures, J. Appl. Cryst. 26 (1993) 283–291.
[38] M.J. Sippl, Recognition of errors in three-dimensional structures of proteins, Proteins 17 (1993) 355–362.

[39] E.F. Pettersen, T.D. Goddard, C.C. Huang, G.S. Couch, D.M. Greenblatt, E.C. Meng, T.E. Ferrin, UCSF Chimera—a visualization system for exploratory research and analysis, J. Comput. Chem. 25 (2004) 1605–1612.
[40] W.S. Delano, The PyMOL Molecular Graphics System, Delano Scientific, San Carlos, CA, 2002, http://www.pymol.org.
[41] S. Swenson, F.S. Markland Jr., Snake venom fibrin(ogen)olytic enzymes, Toxicon 45 (2005) 1021–1039.
[42] C.F. Toombs, Alfimeprase: pharmacology of a novel fibrinolytic metalloproteinase for thrombolysis, Haemostasis 31 (2001) 141–147.
[43] R.O. Hynes, Integrins: versatility, modulation, and signaling in cell adhesion, Cell 69 (1992) 11–25.
[44] W.J. Wang, C.H. Shi, T.F. Huang, Primary structure and antiplatelet mechanism of a snake venom metalloproteinase, acurhagin, from *Agkistrodon acutus* venom, Biochimie 87 (2005) 1065–1077.
[45] J.J. Calvete, M.P. Moreno-Murciano, L. Sans, M. Jurgens, M. Schrader, M. Raida, D.C. Benjamin, J.W. Fox, The disulfide bond pattern of catrocollastin C, a disintegrin-like/cysteine-rich protein isolated from *Crotalus atrox* venom, Protein Sci. 9 (2000) 1365–1373.
[46] A.S. Kamiguti, M. Zuzel, R.D.G. Theakston, Snake venom metalloproteinases and disintegrins: interactions with cells, Braz. J. Med. Biol. Res. 31 (1998) 853–862.
[47] W.-J. Wang, C.-H. Shih, T.-F. Huang, Primary structure and antiplatelet mechanism of a snake venom metalloproteinase, acurhagin, from *Agkistrodon acutus* venom, Biochimie 87 (2002) 1065–1077.
[48] Y. Kubota, R. Kuroki, K. Nishiwaki, A fibulin-1 homolog interacts with an ADAM protease that controls cell migration in *C. elegans*, Curr. Biol. 14 (2004) 2011–2018.
[49] B. Podbilewicz, ADM-1, a protein with metalloprotease- and disintegrin-like domains, is expressed in syncytial organs, sperm, and sheath cells of sensory organs in *Caenorhabditis elegans*, Mol. Biol. Cell 7 (1996) 1877–1893.
[50] X. Zhu, M. Teng, L. Niu, Structure of acutolysin-C, a haemorrhagic toxin from the venom of *Agkistrodon acutus*, providing further evidence for the mechanism of the pH-dependent proteolytic reaction of zinc metalloproteinases, Acta Crystallogr. 55D (1999) 1834–1841.
[51] K.F. Huang, S.H. Chiou, T.P. Ko, J.M. Yuann, A.H. Wang, The 1.35 Å structure of cadmium-substituted TM-3, a snake-venom metalloproteinase from Taiwan habu: elucidation of a TNF-converting enzyme-like active-site structure with a distorted octahedral geometry of cadmium, Acta Crystallogr. 58D (2002) 1118–1128.
[52] L. Watanabe, J.D. Shannon, R.H. Valente, A. Rucavado, A. Alape-Girón, A.S. Kamiguti, R.D.G. Theakston, J.W. Fox, J.M. Gutiérrez, R.K. Arni, Amino acid sequence and crystal structure of BaP1, a metalloproteinase from *Bothrops asper* snake venom that exerts multiple tissue-damaging activities, Protein Sci. 12 (2003) 2273–2281.
[53] W. Stöcker, F. Grams, U. Baumann, P. Reinemer, F.X. Gomis-Ruth, D.B. McKay, W. Bode, The metzincins-topological and sequential relations between the astacins, adamalysins, serralysins, and matrixins (collagenases) define a siperfamily of zinc-peptidases, Protein Sci. 4 (1995) 823–840.